Effect of bulk dispersion on the electron–optical-phonon interaction in a single quantum well

N. C. Constantinou and B. K. Ridley
Department of Physics, University of Essex, Colchester C04 3SQ, England
(Received 28 February 1994)

The interaction of electrons with GaAs optical phonons is investigated for a single GaAs/AlAs quantum well using the hybrid model of optical phonons, which incorporates bulk-mode dispersion. We predict resonances in the individual hybrid scattering rates as a function of well width corresponding to wave vectors where the modes anticross. Nevertheless, although the physics is quite different, we find that the total scattering rate is insensitive to the value of the bulk dispersion, and is given to an excellent approximation by the dielectric continuum model, for both intrasubband and intersubband scattering processes. We conclude, in accord with recent results of lattice dynamics, that for the evaluation of scattering rates, the dielectric continuum model provides a very good approximation.

I. INTRODUCTION

The interaction of electrons with the optical modes in quantum wells and superlattices is of central importance for the properties of these quasi-low-dimensional structures, providing the principal mechanism for energy relaxation at carrier temperatures above about 40 K and for capture of electrons into the wells. It is essential for the accurate modeling of devices like the hot-electron transistor, the quantum-well laser, and the quantum-well infrared detector, that both intrasubband and intersubband scattering rates via the interaction with optical phonons be well established. *Ab initio* lattice-dynamical calculations of electron-phonon interactions[1] have been carried out recently for the GaAs/AlAs system with the main conclusion being that the dielectric continuum (DC) model, e.g., Refs. 2 and 3, gives an accurate value for the scattering rates, both intrasubband and intersubband scattering. This conclusion is supported by the work of Bhatt *et al.*,[4] where a simplified microscopic model was employed to evaluate the phonon modes. The inference is, therefore, that the so-called hydrodynamic (HD) model[5] is an inappropriate description of the optical modes for calculating scattering rates.

The DC model predicts a set of confined modes (the so-called slab modes) all oscillating at the GaAs LO frequency together with two pairs of interface modes, one pair within the GaAs reststrahl band, and the other pair within the AlAs band.[2,3] The problem with *ab initio* calculations is that they are computationally prohibitive, while the problem with the dielectric continuum (DC) model (although it is comparatively straightforward analytically) is that it ignores mechanical dispersion (instead, employing the Einstein approximation) and mechanical boundary conditions, relying on electrostatic boundary conditions to achieve the well-established phenomenon[6,7] of optical-phonon confinement in the GaAs/AlAs system. These approximations are inconsistent with Raman measurements and more recent micro-Raman studies. In particular, the DC model cannot predict the zone-center anisotropy recently observed experimentally.[8,9] Nevertheless, attempts to incorporate mechanical boundary conditions within the dielectric continuum framework have been carried out notably by Huang and Zhu[10] and Nash and Mowbray,[11] although still within the Einstein approximation. It was shown recently by Nash[12] that any such attempt will lead to the total scattering rate being invariant to any change of model (the rate being the same as that predicted by the DC model) provided the set of modes are complete and orthogonal. This is an important conclusion, and has consequences for phonon band structure engineering as discussed by Nash.[12] It should be noted here that this conclusion assumes that the confined modes are dispersionless.

In this paper we consider the electron-phonon interaction in a single well, modeling the optical phonons within the so-called hybrid model.[13,14] This continuum model has the desirable features of obeying *both* electrostatic and mechanical boundary conditions, and is in effect a fusion of the DC and HD models. It includes bulk phonon dispersion and agrees with both lattice dynamics[15] and state of the art Raman measurements.[7,16] As such we can be confident that this continuum model is a close approximation to reality, both for small (the Raman regime) and large wave vectors (the electron–optical-phonon scattering regime). We employ this model to determine what effect, if any, bulk mode dispersion has on the rates. Further, a detailed comparison of the predictions of the hybrid model with those of the DC model (which is known from lattice dynamics[1,4] to be very accurate at the large wave vectors of interest) has not been given before, to our knowledge, although a partial comparison was made in Ref. 14. The effect of mechanical dispersion on the interaction, to our knowledge, also has not been attempted before.

We shall consider only the interaction of electrons with the well modes. The interaction of the carriers with the AlAs interface mode, although important,[2,3] should not be too greatly influenced by dispersion since dispersion is small in AlAs and not enough to hybridize all the modes within the AlAs reststrahl band. This is in contrast to GaAs, where the dispersion is greater and hybridization occurs throughout the reststrahl band. Any effect on the

scattering rates due to bulk dispersion would therefore be more readily apparent in the interaction with the well modes, and we therefore only consider these in this paper.

II. THE DISPERSION OF OPTICAL HYBRID MODES

We consider a single GaAs well of width d ($|z| \leq d/2$) surrounded by AlAs ($|z| > d/2$), the coordinate system is such that the z axis is normal to the layers and the direction of propagation can be taken without loss of generality to be the x axis. The GaAs material parameters are labeled by 1, and those of AlAs by 2 (their values are as given by Adachi[17]). The reduced ionic displacement field $\mathbf{u}$ satisfies the following wave equation[5,12–16,18,19] which was first proposed by Babiker:[5]

$$\ddot{\mathbf{u}} = b_{11}\mathbf{u} + b_{12}\mathbf{E} - v_L^2 \nabla(\nabla\cdot\mathbf{u}) + v_T^2 \nabla\times(\nabla\times\mathbf{u}) , \tag{1}$$

$$\mathbf{P} = b_{12}\mathbf{u} + b_{22}\mathbf{E} . \tag{2}$$

In the above, $\mathbf{E}$ is the electric field, $\mathbf{P}$ the polarization field, and the b coefficients are the usual Born and Huang coefficients which are not repeated here for brevity, but which may be found elsewhere.[5] The parameters v_L and v_T describe the bulk dispersion of LO and TO modes, and are in principle determined by comparison with experiment.[15,20]

In this work we shall only consider the GaAs modes, and these are confined within the layer and the electrostatic and mechanical boundary conditions appropriate for this system, are as follows:[14,15,18]

$$E_x \text{ and } D_z \text{ continuous} , \tag{3}$$

$$\mathbf{u} = 0 , \tag{4}$$

where $\mathbf{D}$ is the electric displacement field. A unique linear combination (triple hybrids) consisting of a pure LO mode, a pure interface mode, and a TO mode is required in order for all of the above boundary condition to be satisfied.[14,15] This triple hybrid scheme when applied to the superlattice system leads to excellent agreement with lattice-dynamics calculations, as regards the mode frequencies.[15] It was pointed out[15] that the relaxation of the mechanical boundary condition (4) to the requirement that only the normal component of the ionic field vanishes at the boundaries:

$$u_z = 0 , \tag{5}$$

leads to only marginal error in the mode frequencies,[15] and simplifies the problem by dispensing with the need for a TO part of the hybrid, which in any case does not have an electric field associated with it, and does not therefore contribute to the Frohlich coupling mechanism. The approximate boundary condition given by Eq. (5) is equivalent to assuming that $\nabla\times\mathbf{u}=0$ identically. With this approximation, only the hybridization of LO and interface modes need be considered, leading to double hybrids.[16,21]

We outline the method of forming double optical hybrids. In order for the boundary conditions embodied in Eqs. (3) and (5) to be satisfied, an LO mode must hybridize with an interface mode, and the ionic displacement for the resultant mode is then a linear combination of the two, viz.

$$\mathbf{u} = \mathbf{u}_L + \mathbf{u}_I \quad (\nabla\times\mathbf{u}_L = 0;\ \nabla\cdot\mathbf{u}_I = 0,\ \nabla\times\mathbf{u}_I = 0) \tag{6}$$

(retardation effects are ignored). From symmetry, the modes can be labeled as symmetric (S) or antisymmetric (A) with respect to the plane $z=0$, where the symmetry relates to that of the in-plane component of the modes (the x component). The components of the ionic displacement field within the well for the S and A hybrids are (using the notation $\mathbf{u}=[u_x,0,u_z]$)

$$\mathbf{u}_L^{(S)} = A_L^{(S)} \left[\cos(k_L z), 0, \frac{ik_L}{q}\sin(k_L z) \right] ,$$
$$\mathbf{u}_L^{(A)} = A_L^{(A)} \left[\sin(k_L z), 0, -\frac{ik_L}{q}\cos(k_L z) \right] , \tag{7}$$

$$\mathbf{u}_I^{(S)} = A_I^{(S)}[\cosh(qz), 0, -i\sinh(qz)] ,$$
$$\mathbf{u}_I^{(A)} = A_I^{(A)}[\sinh(qz), 0, -i\cosh(qz)] , \tag{8}$$

where $A_L^{(S,A)}$ and $A_I^{(S,A)}$ are mode amplitudes, q is the in-plane wave vector, and the factor $\exp(iqx-\omega t)$ is dropped throughout for convenience. The confinement wave vector k_L is given by[13–16]

$$\omega^2 = \omega_{L1}^2 - v_L^2(k_L^2 + q^2) . \tag{9}$$

Equation (9) embodies the assumption of parabolic bulk dispersion, which, although not above criticism, yields reliable results for the GaAs/AlAs system.[15,16] The electric fields associated with the hybrid components in the well are given by

$$\mathbf{E}_L^{(j)} = -\rho_0 \mathbf{u}_L^{(j)}, \quad E_I^{(j)} = -\rho_0 s \mathbf{u}_I^{(j)}, \quad j = S, A , \tag{10}$$

where ρ_0 is related to the effective charge density[13,14]

$$\rho_0^2 = \frac{M\omega_{L1}^2}{\varepsilon_0 V_0}\left[\frac{1}{\varepsilon_{\infty 1}} - \frac{1}{\varepsilon_{s1}}\right] , \tag{11}$$

with M the reduced mass, and V_0 the volume of the unit cell (the other symbols have their usual meaning and are those appropriate for GaAs). The frequency-dependent factor s is expressible as[22]

$$s = (\omega^2 - \omega_{T1}^2)(\omega_{L1}^2 - \omega_{T1}^2)^{-1} . \tag{12}$$

In the barrier, for modes with frequencies within the GaAs reststrahl band, we assume that AlAs is mechanically rigid ($\mathbf{u}=0$), although this does not preclude barrier electric fields due to the GaAs hybrids. These fields are given by

$$\mathbf{E}_B^{(S)} = A_B^{(S)}\rho_0 e^{-q|z|}[1, 0, \mathrm{sgn}(z)i] ,$$
$$\mathbf{E}_B^{(A)} = A_B^{(A)}\rho_0 e^{-q|z|}[\mathrm{sgn}(z), 0, i], \quad |z| > \frac{d}{2} , \tag{13}$$

where $\mathrm{sgn}(z)$ denotes the sign of z. The electric displacement field $\mathbf{D}$ is provided solely by the interface component of the hybrid (the electric displacement field associated with the LO component vanishes, i.e., $\mathbf{D}_L = 0$) and

is given by

$$\mathbf{D}^{(j)}=\varepsilon_0\varepsilon_1\mathbf{E}_I^{(j)}, \quad |z|\le\frac{d}{2}\ ,$$
$$\mathbf{D}^{(j)}=\varepsilon_0\varepsilon_2\mathbf{E}_B^{(j)}, \quad |z|>\frac{d}{2}\ , \tag{14}$$

with ε_0 the permittivity of free space, and $\varepsilon_{1(2)}$ the dielectric function of GaAs (AlAs), i.e.,

$$\varepsilon_i=\varepsilon_{\infty i}\frac{\omega^2-\omega_{\mathrm{Li}}^2}{\omega^2-\omega_{\mathrm{Ti}}^2}, \quad i=1,2\ . \tag{15}$$

On applying the boundary conditions [Eqs. (3) and (5)], we obtain the following dispersion relations for the symmetric and antisymmetric modes:[14]

$$\left[\frac{k_L}{q}\right]\tan\left[\frac{k_Ld}{2}\right]+\left[\frac{1}{s\Delta_S}\right]\tanh\left[\frac{qd}{2}\right]=0$$
symmetric modes , (16)

$$\left[\frac{k_L}{q}\right]\cot\left[\frac{k_Ld}{2}\right]-\left[\frac{1}{s\Delta_A}\right]\coth\left[\frac{qd}{2}\right]=0$$
antisymmetric modes , (17)

where Δ_A and Δ_S are expressible as

$$\Delta_S=\varepsilon'\tanh\left[\frac{qd}{2}\right]+1, \quad \Delta_A=\varepsilon'\coth\left[\frac{qd}{2}\right]+1\ , \tag{18}$$

with $\varepsilon'=\varepsilon_1/\varepsilon_2$. It is noted that the vanishing of $\Delta_{S(A)}$ yields the dispersion relation for the pure symmetric (antisymmetric) interface modes.[3,23,24] In what follows we use the term pure to describe interface modes that are not hybridized with LO modes, and their frequencies are given by $\Delta_{S(A)}=0$.

It is worth briefly discussing the limit of zero dispersion ($v_L\to 0$). Two situations arise in this limit. In the first instance we have the situation $\omega\neq\omega_{L1}$, in which case the pure interface modes are recovered, whereas the second possibility gives $\omega=\omega_{L1}$ and we recover the modes described by Nash and Mowbray[11] which are orthogonal and form a complete set.[12] Note that it is not the confined modes of the DC model that are the zero-dispersion limit of the hybrid theory, but rather the confined modes described in Ref. 11. Since the model of Nash and Mowbray gives the same total rate as the DC model,[12] we compare the hybrid theory to the DC model both for its simplicity and the fact that this model has been widely employed.

We illustrate the hybrid dispersion for a well width of 28 Å (corresponding to ten monolayers of GaAs grown along the [100] direction), taking v_L to be 2.8×10^3 ms^{-1}, which is close to the experimental value.[15,20] We note that hybridization is very evident, and the mode behavior illustrates the well-known anticrossings for both odd and even modes (see Fig. 1).

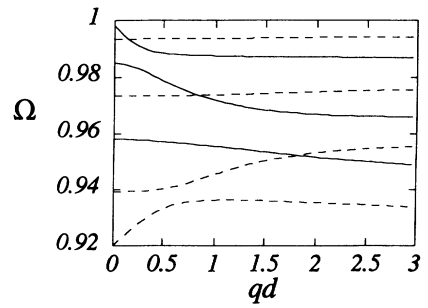

FIG. 1. The hybrid mode frequency $\Omega(=\omega/\omega_{L1})$ as a function of in-plane wave vector qd for $d=28$ Å and $v_L=2.8\times10^3$ ms^{-1}. The full curves correspond to the odd modes, and the dashed curves to the even modes.

III. MODE NORMALIZATION AND THE ELECTRON-PHONON INTERACTION

The mode amplitudes are related via the boundary conditions thus:

$$A_I^{(S)}=-\frac{\cos\left[\frac{k_Ld}{2}\right]}{s\cosh\left[\frac{qd}{2}\right]}A_L^{(S)}\ ,$$
$$A_B^{(S)}=-\left[\frac{\varepsilon'}{\Delta_S}\right]e^{qd/2}\cos\left[\frac{k_Ld}{2}\right]\tanh\left[\frac{qd}{2}\right]A_L^{(S)}\ , \tag{19}$$
$$A_I^{(A)}=-\frac{\sin\left[\frac{k_Ld}{2}\right]}{s\sinh\left[\frac{qd}{2}\right]}A_L^{(A)}\ ,$$
$$A_B^{(A)}=-\left[\frac{\varepsilon'}{\Delta_A}\right]e^{qd/2}\sin\left[\frac{k_Ld}{2}\right]\coth\left[\frac{qd}{2}\right]A_L^{(A)}\ . \tag{20}$$

We need to determine the unknown amplitudes $A_L^{(j)}$, and this is achieved by equating the mode energy to that of an equivalent harmonic oscillator. The mode energy is given by the following Hamiltonian:

$$\hat{H}=\frac{M}{4V_0}\left[\int\dot{\hat{U}}^2(\mathbf{r},t)d\mathbf{r}+\omega^2\int\hat{\mathbf{U}}^2(\mathbf{r},t)d\mathbf{r}\right]\ , \tag{21}$$

where $\hat{\mathbf{U}}(\mathbf{r},t)$ is the displacement operator for the hybrid modes:

$$\hat{\mathbf{U}}(\mathbf{r},t)=\sum_{\mathbf{q}}(\mathbf{u}a_{\mathbf{q}}+\mathbf{u}^*a_{\mathbf{q}}^\dagger)\ . \tag{22}$$

In the above, $a_{\mathbf{q}}$ ($a_{\mathbf{q}}^\dagger$) is the annihilation (creation) operator, and to obtain the mode amplitudes we equate Eq. (21) with the standard expression for the energy of the oscillator:

$$\hat{H}=\sum_{\mathbf{q}}\hbar\omega(a_{\mathbf{q}}^\dagger a_{\mathbf{q}}+\tfrac{1}{2})\ . \tag{23}$$

This procedure leads to the following result for the am-

plitudes:

$$A_L^{(j)}=\frac{q}{k_L}\left[\frac{\hbar}{MN\omega f_j}\right]^{1/2}, \tag{24}$$

where N is the number of unit cells in the well, and

$$f_S=1+3\frac{\sin(k_Ld)}{k_Ld}+\frac{4}{qd}\sin^2\left[\frac{k_Ld}{2}\right]\coth\left[\frac{qd}{2}\right]+\left[\frac{q}{k_L}\right]^2\left[1+\frac{\sin(k_Ld)}{k_Ld}\right], \tag{25}$$

$$f_A=1-3\frac{\sin(k_Ld)}{k_Ld}+\frac{4}{qd}\cos^2\left[\frac{k_Ld}{2}\right]\tanh\left[\frac{qd}{2}\right]+\left[\frac{q}{k_L}\right]^2\left[1-\frac{\sin(k_Ld)}{k_Ld}\right]. \tag{26}$$

In obtaining the above normalization of the mode amplitudes, we ignored the small electrical component of the energy which resides in the AlAs region. The energy of the optical mode is dominated by the mechanical part.[14]

With all the mode amplitudes now determined, we may proceed to describe the interaction of the electrons with the hybrids. We chose to work entirely with scalar potentials, as this has been shown to be appropriate for evaluating the rates.[24] The electrostatic potentials associated with the hybrids are given by

$$\hat{\mathbf{E}}_j=-\nabla\hat{\Phi}_j,\quad j=S,A. \tag{27}$$

Explicitly, the potentials are given by the following expression:

$$\hat{\Phi}_j=\sum_{\mathbf{q}}(\phi_j a_q+\phi_j^* a_{\mathbf{q}}^\dagger), \tag{28}$$

where

$$\phi_S=-i\frac{\rho_0 A_L^{(S)}}{q}\left\{\cos(k_Lz)+s\left[\frac{k_L}{q}\right]\frac{\sin(k_Ld/2)}{\sinh(qd/2)}\times\cos(qz)\right\},\quad |z|\le\frac{d}{2} \tag{29a}$$

$$\phi_S=\frac{i}{q}A_B^{(S)}\rho_0 e^{-q|z|},\quad |z|>\frac{d}{2}, \tag{29b}$$

$$\phi_A=-i\frac{\rho_0 A_L^{(A)}}{q}\left\{\sin(k_Lz)-s\left[\frac{k_L}{q}\right]\frac{\cos(k_Ld/2)}{\cosh(qd/2)}\times\sinh(qz)\right\},\quad |z|\le\frac{d}{2} \tag{30a}$$

$$\phi_A=\frac{i}{q}A_B^{(A)}\rho_0 e^{-q|z|}\mathrm{sgn}(z),\quad |z|>\frac{d}{2}. \tag{30b}$$

The interaction Hamiltonian is then of the usual Frohlich type:

$$\hat{H}_{\mathrm{int}}^{(j)}=-e\hat{\Phi}_j. \tag{31}$$

The electrons are assumed to be confined by an infinite potential, and the electronic states are therefore

$$\Psi_n=\left[\frac{2}{V}\right]^{1/2}e^{ikx}\begin{cases}\cos\left[\frac{n\pi}{d}\right], & n=1,3,5\ldots\\ \sin\left[\frac{n\pi}{d}\right], & n=2,4,6,\ldots,\end{cases}$$
$$E_n=\frac{n^2\hbar^2\pi^2}{2m^*d^2}, \tag{32}$$

where k is the in-plane electronic wave vector, E_n the subband energy, and $V(=NV_0)$ is the volume of the slab. The scattering rate is obtainable via Fermi's golden rule (we consider only the low-temperature emission rates):

$$\Gamma=\frac{2\pi}{\hbar}\sum_{k_L}\sum_{\mathbf{q}}|\langle f|\hat{H}_{\mathrm{int}}^{(j)}|i\rangle|^2\delta(E_f-E_i), \tag{33}$$

where $i(f)$ refers to the initial (final) combined electron-phonon state.

A. Intrasubband rates

We first consider scattering processes within the first subband. From symmetry considerations only the symmetric hybrids contribute. In general, the rates have to be computed numerically. We will, however, focus attention on threshold rates in which the electron has just enough energy to emit a mode. For parabolic bands this implies that the in-plane wave vector of the electron is given by

$$k_0=\left[\frac{2m^*\omega_{L1}}{\hbar}\right]^{1/2}, \tag{34}$$

with m^* the GaAs effective mass ($k_0\approx 2.4\times10^6$ cm^{-1}). It is instructive to investigate the hybrid frequencies as a function of well width for *fixed* $q(=k_0)$; this dependence is illustrated in Fig. 2. We find a rich structure in the hybrid dispersion. Concentrating on the even modes, the

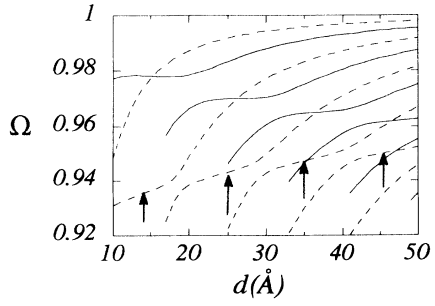

FIG. 2. Hybrid mode frequency $\Omega(=\omega/\omega_{L1})$ as a function of well width d for fixed threshold wave vector $q=2.4\times10^6$ cm^{-1}. The full curves correspond to the odd modes, and the dashed curves to the even modes. The arrows indicate the points at which the resonances occur in Fig. 3.

first point to notice is that the number of modes depends on the well width; the larger the well width the larger the number. The second point is that the regions of the various curves marked by an arrow correspond to the range in which the hybrid is most like the pure interface mode, i.e., to the anticrossing region. The same observations apply to the odd-order hybrids, although of course they do not participate in intrasubband events.

Returning to the actual intrasubband threshold rates, the following analytic result is obtained:

$$\Gamma=2(2\pi)^6\Gamma_0\left[\frac{\hbar\omega_{L1}}{E_1}\right]^{1/2}\sum_{k_L}\frac{\sin^2(k_L d/2)}{(k_L d)^4 f_S}\left\{\frac{1}{4\pi^2-(k_L d)^2}+\left[\frac{k_L}{k_0}\right]^2\left[\frac{s}{4\pi^2+(k_0 d)^2}\right]\right\}^2, \tag{35}$$

with Γ_0 ($\approx 8.7\times10^{12}$ s^{-1} for GaAs) related to the Frohlich coupling constant α via

$$\Gamma_0=2\omega_{L1}\alpha=\frac{e^2}{4\pi\varepsilon_0\hbar}\left[\frac{2m^*\omega_{L1}}{\hbar}\right]^{1/2}\left[\frac{1}{\varepsilon_{\infty 1}}-\frac{1}{\varepsilon_{s1}}\right]. \tag{36}$$

The above intrasubband rate is depicted in Fig. 3 as a function of well width. As a comparison we also plot the predictions of the DC model (the relevant scattering rates for the DC model are listed in the Appendix). We see that the total rates are practically identical for the two models, with only a very marginal difference at small well widths. The contribution to the total rate of the DC model arises via scattering by confined (slab) modes and the symmetric GaAs interface mode. The contribution from the individual hybrids shows some interesting properties. First, the number of hybrids varies with well width for the reasons outlined previously. Hence, as the well width increases, an additional mode becomes available for scattering. Further we predict resonances at well widths corresponding to the flat parts of the curves in Fig. 2. Finally, we find that the total intrasubband hybrid rate is insensitive to the value of v_L. The variation in the scattering rate with v_L for a fixed well width (=28 Å) is illustrated in Fig. 4. For a value of v_L greater than 2.8×10^3, the number of modes within the reststrahl band of GaAs decreases (for example, a value for v_L of 3.8×10^3 ms^{-1} corresponds to a [111] growth direction[15]). Hence a plot analogous to Fig. 3 would result in fewer resonances, since the number of even modes within the reststrahl band is reduced, although as illustrated in Fig. 4 the total rate hardly changes. For values less than v_L around 2×10^3 ms^{-1} the dispersion may be too small for hybridization to be effective across the entire reststrahl band, and the interface mode will be pure in this case with the contribution given accordingly from a nondispersive model (see the Appendix). Even in this case, the scattering rate will not change. The point $v_L=0$ in Fig. 4 corresponds to the DC value, as of course it must.

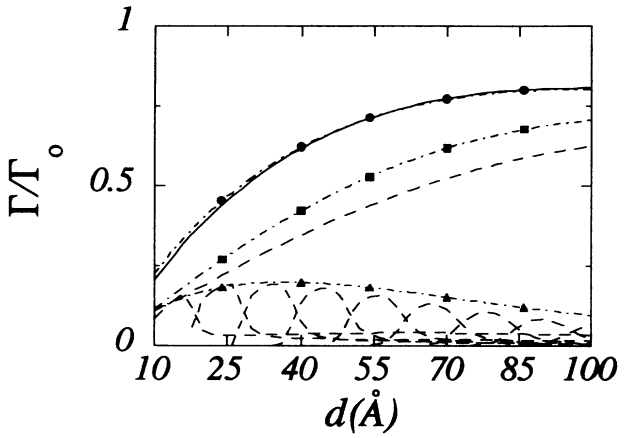

FIG. 3. The threshold intrasubband scattering rate as a function of well width d. The solid curve corresponds to the total rate calculated via the hybrid model with $v_L=2.8\times10^3$ ms^{-1}, and the dashed curves are the contribution to this from the individual hybrid modes. The dot-dashed curve marked by circles corresponds the total rate calculated via the DC model; the contributions to this are made up of confined slab modes (dot-dashed curve with squares) and the pure GaAs interface modes (dot-dashed curve with triangles).

B. Intersubband scattering

For intersubband scattering, we consider an electron at the bottom of the second subband (zero initial in-plane wave vector), which then scatters to the first subband by emitting an antisymmetric hybrid. Conservation of momentum then entails that the resultant electronic in-plane wave vector is given by

$$\tilde{k}_0=k_0\left[\frac{E_2-E_1}{\hbar\omega_{L1}}-1\right]^{1/2}. \tag{37}$$

We note that this wave vector is quite large for small well widths, and approaches zero as $E_2-E_1\rightarrow\hbar\omega_{L1}$. The scattering rate for this intersubband process is given in closed form by the following expression:

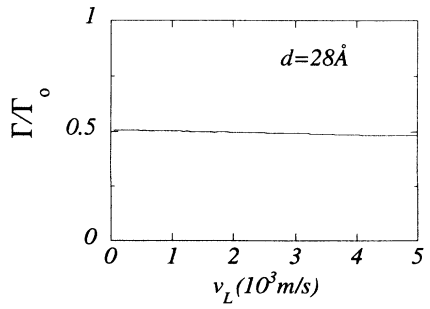

FIG. 4. The threshold intrasubband scattering rate as a function of v_L for $d=28$ Å.

$$\Gamma=2^9\pi^6\Gamma_0\left[\frac{\hbar\omega_{L1}}{E_1}\right]^{1/2}\sum_{k_L}\frac{\cos^2(k_Ld/2)}{f_A}\left\{\frac{1}{[\pi^2-(k_Ld)^2][9\pi^2-(k_Ld)^2]}-\frac{s}{[\pi^2+(\tilde{k}_0d)^2][9\pi^2+(\tilde{k}_0d)^2]}\right\}^2. \quad (38)$$

Figure 5 illustrates the intersubband rate as a function of well width (the smallest well width considered is 50 Å, in order to ensure a second confined state and the validity of the infinite well approximation, which breaks down for small well widths). Again the agreement for the total rates obtained from Eq. (38), and that given by the DC model (see the Appendix) is excellent. It is noted that the contribution given by the pure antisymmetric interface mode to the DC rate is rather small for intersubband scattering. Nevertheless, it can be seen from the inset to Fig. 5 that the corresponding contributions from the hybrid theory again show resonances analogous to those in the intrasubband rate. In both the hybrid and DC models, the dominant contribution to the intersubband rate is due to the highest energy antisymmetric hybrid, and the $n=2$ slab mode (see the Appendix).

Again, in analogy with the intrasubband results, the intersubband rates are insensitive to the value of the bulk dispersion.

IV. CONCLUSIONS

Our aim in this paper was to investigate the role played by mode dispersion in electron-phonon interactions. We applied the hybrid continuum model of confined polar optical phonons, which incorporates mode dispersion in a natural way, to determine both intrasubband and intersubband scattering rates, and concentrated on the interaction with GaAs modes. The main conclusion of this work is that the rates obtained via the simple DC model are in excellent agreement with those obtained by the hybrid model, irrespective of the value of the bulk dispersion. This result agrees with the conclusions of lattice dynamics,[1,2,4] and the conclusions originally made by Nash and Mowbray.[11] Nevertheless, the details are quite different, and we predict resonances in the rates as a function of well width in the wave-vector region where the hybrids have a substantial interface mode component. These resonances, as far as we are aware, have not been discussed before in detail, although Tsuchiya and Ando[25] show structure in the polaron damping rate which they attribute to the change in the number of modes as the well width changes. It is noted that the model employed by Tsuchiya and Ando also yields results in close agreement with the DC model.

Finally we discuss the relevance of our results to the aim of modifying the electron–optical-phonon interaction in layered media. It is of obvious technological advantage to be able to reduce the electron–optical-phonon interaction. Some recent work on modifying the electron-phonon interactions have been carried out, and we briefly mention them here.

By the use of metal/semiconductor junctions,[26–29] it has been demonstrated that the important interface modes are modified in such devices, and this leads to a predicted reduction in the scattering rates.[27–29] Another interesting approach considered by Bechstedt, Grille, and Haupt[30] is the modification of the phonon modes in parabolic quantum wells fabricated with semiconductor alloys. All of these investigations involve the alteration of the phonon properties. In contrast, Tsuchiya and Ando[31] considered structures which resulted in a modification of the electronic states, which in turn alters the electron phonon interaction and hence the high-temperature mobilities. The conclusion of our work suggest that choosing materials in order that bulk mode dispersion is either greater or less than that of GaAs will have only a very marginal effect on the electron-phonon interaction, assuming of course that all other factors remain equal (such as the TO-LO splitting, for example).

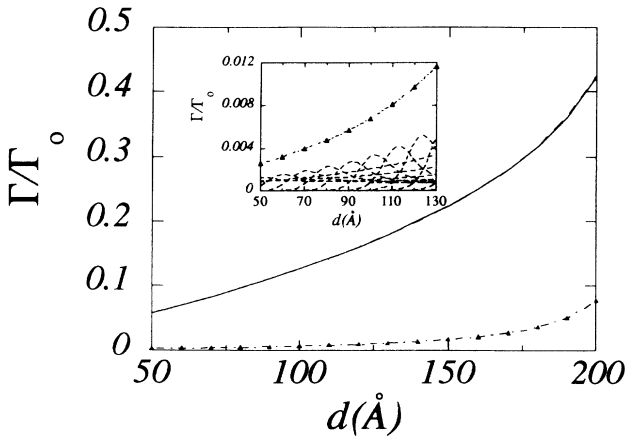

FIG. 5. The intersubband scattering rate as a function of well width d. The solid curve is the total rate via antisymmetric hybrids, while the dashed curve is the total rate calculated via the DC model (the slab plus the GaAs interface mode). The dot-dashed curve marked by triangles is the contribution to the total DC rate from the pure GaAs interface mode. The inset depicts the resonances predicted by the hybrid model for the higher-order hybrids.

ACKNOWLEDGMENTS

We thank Dr. M. Babiker for useful discussions, and the Science and Engineering Research Council for financial support under Grant No. GR/J80269.

APPENDIX

In this appendix we quote the various scattering rates deduced via the DC model; the details of these calculations may be found elsewhere.[3,24] The threshold intrasubband rate via emission of symmetric slab modes is given by

$$\Gamma=8\Gamma_0\left[\frac{\hbar\omega_{L1}}{E_1}\right]^{1/2}\times\sum_{n=1,3,5,\ldots}\left[\left\{\frac{1}{n}+\frac{n}{4-n^2}\right\}^2\frac{1}{(k_0d)^2+(n\pi)^2}\right], \tag{A1}$$

with the dominant contribution given by the $n=1$ slab mode. The intersubband rate via antisymmetric slab modes is

$$\Gamma=8\Gamma_0\left[\frac{\hbar\omega_{L1}}{E_1}\right]^{1/2}\times\sum_{n=2,4,6,\ldots}\left\{\left[\frac{1}{n^2-9}-\frac{1}{n^2-1}\right]^2\frac{n^2}{(\tilde{k}_0d)^2+(n\pi)^2}\right\}, \tag{A2}$$

and here the dominant contribution is the $n=2$ mode. The analogous scattering rates via the interaction with the symmetric GaAs interface mode is given by

$$\Gamma=2^5\pi^6\Gamma_0\left[\frac{\omega_{L1}}{\omega}\right]\left[\frac{\hbar\omega_{L1}}{E_1}\right]^{1/2}\frac{s^2\tanh(k_0d/2)}{(k_0d)^3[(k_0d)^2+4\pi^2]^2} \tag{A3}$$

for the intrasubband rate, and

$$\Gamma=2^7\pi^6\Gamma_0(\tilde{k}_0d)\left[\frac{\omega_{L1}}{\omega}\right]\left[\frac{\hbar\omega_{L1}}{E_1}\right]^{1/2}\times\frac{s^2\coth(\tilde{k}_0d/2)}{\{(\tilde{k}_0d)^2+\pi^2\}^2\{(\tilde{k}_0d)^2+9\pi^2\}^2} \tag{A4}$$

for the intersubband scattering rate via the antisymmetric GaAs interface mode.

[1] H. Rucker, E. Molinari, and P. Lugli, Phys. Rev. B **44**, 3463 (1991); **45**, 6747 (1992).
[2] L. Wendler, Phys. Status Solidi B **129**, 513 (1985).
[3] N. Mori and T. Ando, Phys. Rev. B **40**, 6175 (1989).
[4] A. R. Bhatt, K. W. Kim, M. A. Stroscio, and J. M. Higman, Phys. Rev. B **48**, 14 671 (1993).
[5] M. Babiker, J. Phys. C **19**, 683 (1986); B. K. Ridley, Phys. Rev. B **39** 5282 (1989); B. K. Ridley and M. Babiker, *ibid.* **43**, 9096 (1991).
[6] A. K. Sood, J. Menendez, M. Cardona, and K. Ploog, Phys. Rev. Lett. **54**, 2111 (1985); **54**, 2115 (1985).
[7] A. J. Shields, M. Cardona, and K. Eberl, Phys. Rev. Lett. **72**, 412 (1994).
[8] G. Scamarcio, M. Haines, G. Abstreiter, E. Molinari, S. Baroni, A. Fischer, and K. Ploog, Phys. Rev. B **47**, 1483 (1993).
[9] M. Haines and G. Scamarcio, *Phonons in Semiconductor Nanostructures* Vol. 236 of *NATO Advanced Study Institute, Series E,* edited by J-P Leburton *et al.* (Kluwer Academic, Netherlands, 1993), p. 93.
[10] K. Huang and B. Zhu, Phys. Rev. B **38**, 13 377 (1988).
[11] K. J. Nash and D. J. Mowbray, J. Lumin. **44**, 315 (1989).
[12] K. J. Nash, Phys. Rev. B **46**, 7723 (1992).
[13] B. K. Ridley, Phys. Rev. B **44**, 9002 (1991).
[14] B. K. Ridley, Proc. SPIE **1675**, 492 (1992); Phys. Rev. B **47**, 4592 (1993).
[15] M. P. Camberlain, M. Cardona, and B. K. Ridley, Phys. Rev. B **48**, 14 356 (1993).
[16] N. C. Constantinou, O. Al-Dossay, and B. K. Ridley, Solid State Comm. **86**, 191 (1993); **87**, 1087(E) (1993).
[17] S. Adachi, J. Appl. Phys. **58**, R1 (1985).
[18] C. Trallero-Giner, F. Garcia-Moliner, V. R. Velasco, and M. Cardona, Phys. Rev. B **45**, 11944 (1992).
[19] R. Perez-Alvarez, F. Garcia-Moliner, V. R. Velasco, and C. Trallero-Giner, J. Phys. Condens. Matter **5**, 5389 (1993).
[20] D. Strauch and B. Dorner, J. Phys. Condens. Matter **2**, 1457 (1990).
[21] X. Zianni, P. N. Butcher, and I. Dharssi, J. Phys. Condens. Matter **4**, L77 (1992).
[22] B. K. Ridley, *Quantum Processes in Semiconductors,* 2nd ed. (Clarendon, Oxford, 1982), Chap. 9.
[23] O. Al-Dossary, M. Babiker, and N. C. Constantinou, Semicond. Sci. Technol. B **7**, 91 (1992).
[24] M. Babiker, N. C. Constantinou, and B. K. Ridley, Phys. Rev. B **48**, 2236 (1993).
[25] T. Tsuchiya and T. Ando, Phys. Rev. B **47**, 7240 (1993).
[26] L. Wendler, R. Haupt, and V. G. Grigoryan, Physica B **167**, 91 (1990).
[27] M. A. Stroscio, K. W. Kim, G. J. Iafrate, M. Datta, and H. L. Grubin, Philos. Mag. Lett. **65**, 173 (1992).
[28] N. C. Constantinou, Phys. Rev. B **48**, 11 931 (1993).
[29] A. R. Bhatt, K. W. Kim, M. A. Stroscio, G. J. Iafrate, M. Dutta, H. L. Grubin, R. Haque, and X. T. Zhu, J. Appl. Phys. **73**, 2338 (1993).
[30] F. Bechstedt, H. Grille, and R. Haupt, Phys. Rev. B **48**, 14 667 (1993).
[31] T. Tsuchiya and T. Ando, Phys. Rev. B **48**, 4599 (1993).